Appendix 1

Some integrals of the terms A_s, A_η, and A_p defined in (15) and (17*a*), occurring in equation (19*a*) for 3D viscosity variations of the expected values $EX[\eta_T(\alpha_1,\alpha_2,\alpha_3)]$, have the following form:

$$\int_0^{EX(\varepsilon_T)} A_s(\alpha_1,\alpha_2,\alpha_3)d\alpha_2 \equiv \frac{\int_0^{EX(\varepsilon_T)}\left(\int_0^{\alpha_2}\frac{1}{EX(\eta_T)}d\alpha_2\right)d\alpha_2}{\int_0^{EX(\varepsilon_T)}\frac{1}{EX(\eta_T)}d\alpha_2},$$

$$\int_0^{EX(\varepsilon_T)} A_\eta(\alpha_1,\alpha_2,\alpha_3)d\alpha_2 \equiv$$

$$\int_0^{EX(\varepsilon_T)}\left(\int_0^{\alpha_2}\frac{\alpha_2}{EX(\eta_T)}d\alpha_2\right)d\alpha_2 \qquad (A1.1)$$

$$-\left[\frac{\int_0^{EX(\varepsilon_T)}\left(\int_0^{\alpha_2}\frac{1}{EX(\eta_T)}d\alpha_2\right)d\alpha_2}{\int_0^{EX(\varepsilon_T)}\frac{1}{EX(\eta_T)}d\alpha_2}\right]\cdot\left(\int_0^{EX(\varepsilon_T)}\frac{\alpha_2}{EX(\eta_T)}d\alpha_2\right),$$

Here, a particular case has been considered for 2D viscosity variations, where the expected value of the bio-fluid dynamic viscosity $EX[\eta_T(\alpha_1,\alpha_3)]$ has a constant value in gap height direction α_2. Hence the following equations (15), (17a), and (A1.1) can be derived:

$$A_s = \frac{\alpha_2}{EX(\varepsilon_T)} \equiv s, \quad \int_0^{EX(\varepsilon_T)} A_s d\alpha_2 = \frac{EX(\varepsilon_T)}{2}, \quad A_\eta = \frac{EX(\varepsilon_T^2)}{2EX(\eta_T)}(s^2-s),$$

$$\int_0^{EX(\varepsilon_T)} A_\eta d\alpha_2 = -\frac{EX(\varepsilon_T^3)}{12EX(\eta_T)}. \qquad (A1.2)$$

Further, the equations (17b) and (A1.2)can be derived as follows:

$$A_{\rho 1} = \frac{EX(\varepsilon_T^6)}{240\cdot EX(\eta_T^3)}(-s+5s^4-6s^5+2s^6)$$
$$= \frac{EX(\varepsilon_T^6)}{240\cdot EX(\eta_T^3)}s(s-1)\cdot(1+s+s^2-4s^3+2s^4)\ ,$$

$$A_{\rho 2}=\frac{EX(\varepsilon_T^4)}{120\cdot EX(\eta_T^2)}(3s-10s^3+10s^4-3s^5)$$
$$=\frac{EX(\varepsilon_T^4)}{120\cdot EX(\eta_T^2)}s(s-1)(-3-3s+7s^2-3s^3)\ ,$$
$$A_{\rho 3}=\frac{EX(\varepsilon_T^2)}{12\cdot EX(\eta_T)}(-3s+6s^2-4s^3+s^4)=\frac{EX(\varepsilon_T^2)}{12\cdot EX(\eta_T)}s(s-1)\cdot(3-3s+s^2)\ ,\quad (A1.3)$$

$$\int_0^{EX(\varepsilon_T)} A_{\rho 1}d\alpha_2=-\frac{EX(\varepsilon_T^7)}{1120\cdot EX(\eta_T^3)},\ \int_0^{EX(\varepsilon_T)} A_{\rho 2}d\alpha_2=\frac{EX(\varepsilon_T^5)}{240\cdot EX(\eta_T^2)},$$
$$\int_0^{EX(\varepsilon_T)} A_{\rho 3}d\alpha_2=-\frac{EX(\varepsilon_T^3)}{40\cdot EX(\eta_T)},\quad (A1.4)$$

for: $0\le h_1\alpha_1\le 2a$, $-b\le h_3\alpha_3\le b$, $0\le\alpha_2\le EX(\varepsilon_T)$, and $0\le s\le 1$.

Appendix 2

Some derivatives of the terms A_s, A_η. A_p defined in (15) and (17ab), occurring in equation (21) for 3D viscosity variations of expected values $EX[\eta_T(\alpha_1,\alpha_2,\alpha_3)]$ have the following form:

$$\frac{\partial A_s(\alpha_1,\alpha_2,\alpha_3)}{\partial\alpha_2}\equiv\frac{1}{EX(\eta_T)}\cdot\frac{1}{\int_0^{EX(\varepsilon_T)}\frac{1}{EX(\eta_T)}d\alpha_2},\ \frac{\partial A_\eta(\alpha_1,\alpha_2,\alpha_3)}{\partial\alpha_2}\equiv\frac{\alpha_2}{EX(\eta_T)}\ -\frac{1}{EX(\eta_T)}\frac{\int_0^{EX(\varepsilon_T)}\frac{\alpha_2}{EX(\eta_T)}d\alpha_2}{\int_0^{EX(\varepsilon_T)}\frac{1}{EX(\eta_T)}d\alpha_2},\quad (A2.1)$$

whereas the first derivative of equation (17a) with respect to the variable α_2 is as follows:

$$\frac{\partial A_p}{\partial\alpha_2}\equiv\left(\frac{1}{h_1}\frac{\partial EX(p)}{\partial\alpha_1}-M_1\right)^2\frac{\partial}{\partial\alpha_2}\left[A_{\rho 1}(\alpha_1,\alpha_2,\alpha_3)\right]$$
$$-2U_1\left(\frac{\partial EX(p)}{\partial\alpha_1}-h_1M_1\right)\frac{\partial}{\partial\alpha_2}\left[A_{\rho 2}(\alpha_1,\alpha_2,\alpha_3)\right]+\quad (A2.2)$$
$$+(U_1)^2\frac{\partial}{\partial\alpha_2}\left[A_{\rho 3}(\alpha_1,\alpha_2,\alpha_3)\right].$$

Based on equations (17b) and (A2.1), the following equations can be obtained:

$$\frac{\partial}{\partial\alpha_2}\left[A_{\rho 1}(\alpha_1,\alpha_2,\alpha_3)\right]\equiv\frac{1}{EX(\eta_T)}\int_0^{\alpha_2} A_\eta^2 d\alpha_2-\frac{\frac{1}{EX(\eta_T)}\int_0^{EX(\varepsilon_T)}\left(\frac{1}{\eta_T}\int_0^{\alpha_2}A_\eta^2 d\alpha_2\right)d\alpha_2}{\int_0^{EX(\varepsilon_T)}\frac{1}{\eta_T}d\alpha_2},\quad (A2.3a)$$

$$\frac{\partial}{\partial\alpha_2}\left[A_{\rho 2}(\alpha_1,\alpha_2,\alpha_3)\right] \equiv \frac{1}{EX(\eta_T)}\int_0^{\alpha_2}(1-A_s)A_\eta d\alpha_2$$
$$-\frac{\frac{1}{EX(\eta_T)}\int_0^{EX(\varepsilon_T)}\left(\frac{1}{EX(\eta_T)}\int_0^{\alpha_2}(1-A_s)A_\eta d\alpha_2\right)d\alpha_2}{\int_0^{EX(\varepsilon_T)}\frac{1}{EX(\eta_T)}d\alpha_2}, \qquad (A2.3b)$$

$$\frac{\partial}{\partial\alpha_2}\left[A_{\rho 3}(\alpha_1,\alpha_2,\alpha_3)\right]$$
$$\equiv \frac{1}{EX(\eta_T)}\int_0^{\alpha_2}(1-A_s)^2 d\alpha_2$$
$$-\frac{\frac{1}{EX(\eta_T)}\int_0^{EX(\varepsilon_T)}\left(\frac{1}{EX(\eta_T)}\int_0^{\alpha_2}(1-A_s)^2 d\alpha_2\right)d\alpha_2}{\int_0^{EX(\varepsilon_T)}\frac{1}{EX(\eta_T)}d\alpha_2}. \qquad (A2.3c)$$

for $0 < \alpha_2 < EX(\varepsilon_T)$.

Further, a particular case has been considered for 2D viscosity variations where the expected value of the bio-oil dynamic viscosity has a constant value in gap height direction. Equations (15), (17a), and (A2.1) for $EX[\eta_T(\alpha_1,\alpha_3)]$ are as follows:

$$\frac{\partial A_s}{\partial\alpha_2} = \frac{1}{EX(\varepsilon_T)}, \frac{\partial A_\eta}{\partial\alpha_2} = \frac{2\alpha_2 - EX(\varepsilon_T)}{2EX(\eta_T)} = \frac{EX(\varepsilon_T)}{2EX(\eta_T)}(2s-1), \qquad (A2.4)$$

$$\frac{\partial A_{\rho 1}}{\partial\alpha_2} = \frac{EX(\varepsilon_T^5)}{240\cdot EX(\eta_T^3)}(-1+20s^3-30s^4+12s^5), \qquad (A2.5)$$

$$\frac{\partial A_{\rho 2}}{\partial\alpha_2} = \frac{EX(\varepsilon_T^3)}{120\cdot EX(\eta_T^2)}(3-30s^2+40s^3-15s^4), \qquad (A2.6)$$

$$\frac{\partial A_{\rho 3}}{\partial\alpha_2} = \frac{EX(\varepsilon_T)}{12\cdot EX(\eta_T)}(-3+12s-12s^2+4s^3), \qquad (A2.7)$$

for: $0 \le h_1\alpha_1 \le 2a$, $-b \le h_3\alpha_3 \le b$, $0 \le \alpha_2 \le EX(\varepsilon_T)$, $0 \le s \le 1$.

Appendix 3

- Symmetrical distribution of density function f_s for spherical surfaces *(h)* is demonstrated in Figure A3.1.

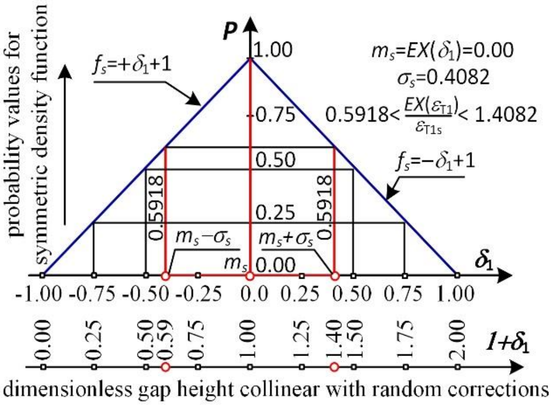

Figure A3.1. The expected value m_s and standard deviation σ_s of the hip gap height (assigned to the upper index *h*) depicted on the symmetrical probability density function f_s with a vertical axis of probability *P*, where the upper horizontal axis provides dimensionless values of the random variable of corrections δ_1 of variations in the joint gap height, the lower horizontal axis represents the dimensionless height of the entire gap $1+\delta_1$. (Figures are elaborated based on the author's measurements and studies)

For the symmetrical function depicted in Figure A3.1, the expected value $m_S^h = 0$ for the random variable of gap height corrections was determined from formula (2). The standard deviation determined from formula (3) provides the value: $\sigma_S^h = 0.4082$. This standard deviation interval was superimposed onto Figure A3.1, on the upper horizontal axis δ_1. In this interval, due to some random changes in the conducted measurements, the random expected value of variations in the gap height may change its location. These changes are assigned a change value of the entire gap, read from the lower horizontal axis $1+\delta_1$, where the dimensionless gap height of 1 is assigned to the value correction δ_1=0 on the upper horizontal axis. Thus, the standard deviation interval and the expected function values (30) of the dimensional height of the entire hip *(h)* gap vary in the following range:

$$\begin{gathered}(m_S^h - \sigma_S^h, m_S^h + \sigma_S^h) = (-0.4082,\ +0.4082\,), \\ 0.5918 \cdot \varepsilon_T(\delta_1 = 0) < EX(\varepsilon_T) < 1.4082 \cdot \varepsilon_T(\delta_1 = 0),\end{gathered} \tag{A3.1}$$

where gap height $\varepsilon_T(\delta = 0) \equiv \varepsilon_0 \cdot \varepsilon_{T1s}(\varphi, \vartheta_1) = \varepsilon_T(\varphi, \vartheta_1, \delta_1 = 0)$. The height of the entire gap may vary. Such changes in the gap height occur with the probability ranging from P_s=0.5918 to P_s=1.0000, represented on the vertical axis in Figure A3.1.

• The two types of unsymmetrical correction parameter density functions describing random variations in the gap height for spherical surfaces (assigned to the upper index *h*) are demonstrated in Figure A3.2a, b and in Figure A3.2c, d.

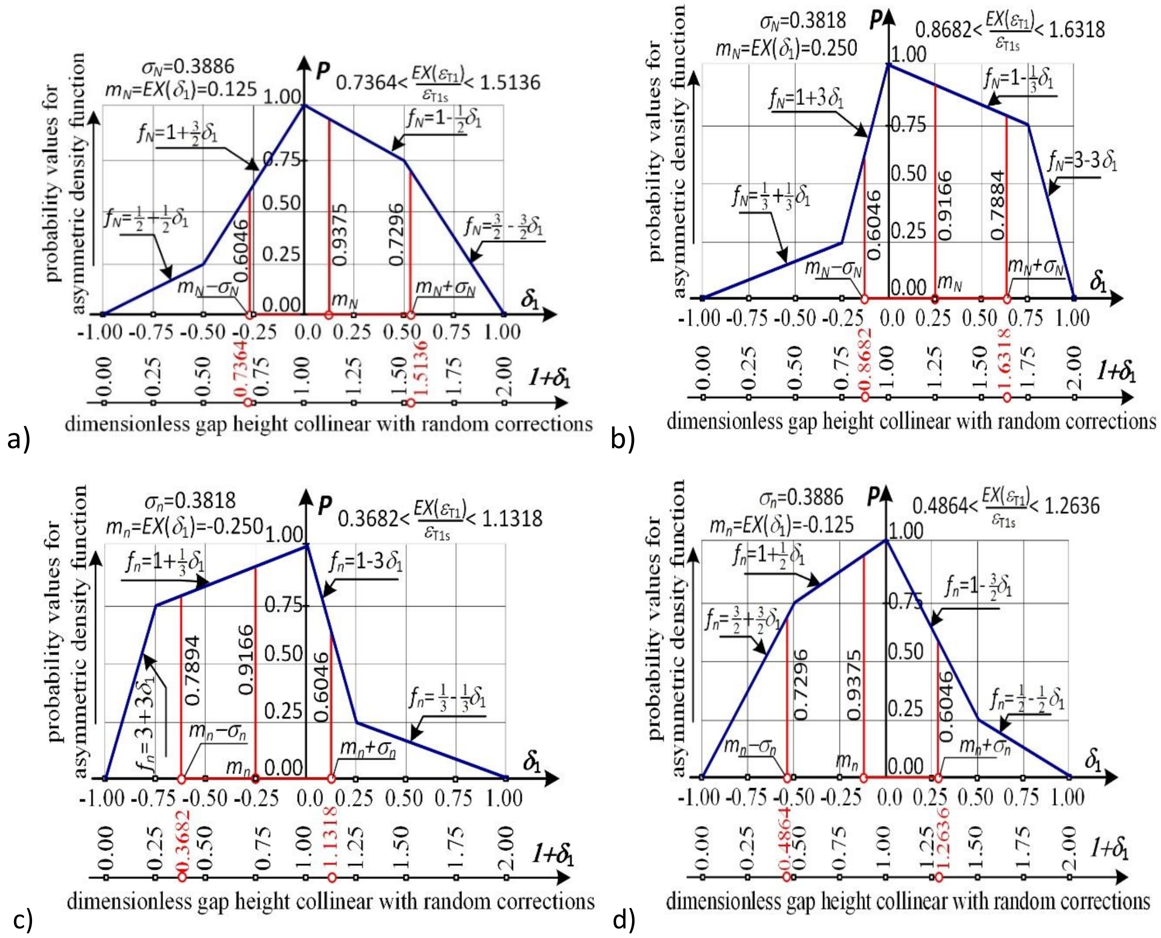

Figure A3.2. The expected values m_N, m_n, and standard deviations σ_N, σ_n of the hip gap height (assigned to the upper index h) depicted on the anti-symmetrical probability density functions: a) for PS, b) for PC: f_N for dominance of random increases over random decreases of the joint gap height, c) for PC, d) for PS: f_n for dominance of random decreases over random increases of joint gap height; where the vertical axis indicates probabilities *P*, the upper horizontal axis represents the dimensionless values of the random variable of increase and decrease corrections of joint gap height δ_1, the lower horizontal axis denotes the heights of the entire gap $1+\delta_1$. (Figures are elaborated based on the author`s studies for PS – Phosphatidylserine and PC – Phosphatidylcholine)

In Figure A3.2 a, b, c, d, the unsymmetrical functions f_N and f_n denote the following expected values for the random variable of gap height corrections for spherical surfaces *(h)* determined by the formula (2): $m_N^h = +0.125$; $m_N^h = +0.250$; $m_N^h = -0.250$; $m_N^h = -0.125$. The standard deviations of the random variable of corrections determined from formula (3) lead to the following values: $\sigma_N^h = 0.3886$; $\sigma_N^h = 0.3818$; $\sigma_n^h = 0.3818$; $\sigma_n^h = 0.3886$. The standard deviation intervals of the random variable of corrections $(m_N^h - \sigma_N^h, m_N^h + \sigma_N^h), (m_n^h - \sigma_n^h, m_n^h + \sigma_n^h)$, were superimposed onto Figure A3.2 a, b, c, d on axis δ_1. In this interval, due to random variations, the random expected value of variations in gap height may change its location. These changes are assigned a change value of the entire gap, read from the collinear second horizontal axis $1+\delta_1$. Thus, the standard deviations intervals and the expected function values (30) of the dimensional height of the entire gap for spherical surfaces *(h)* vary in the following ranges:

$$(-0.2636, +0.5136);\ (-0.1318, +0.6318);\ (-0.6318, +0.1318);\ (-0.5136, +0.2636).\ (A3.2a)$$

$$\begin{aligned}
0.7364 \times \varepsilon T(\delta 1 = 0) \ &< \ EX(\varepsilon T) \ < \ 1.5136 \times \varepsilon T(\delta 1 = 0),\\
0.8682 \times \varepsilon T(\delta 1 = 0) \ &< \ EX(\varepsilon T) \ < \ 1.6318 \times \varepsilon T(\delta 1 = 0),\\
0.3682 \times \varepsilon T(\delta 1 = 0) \ &< \ EX(\varepsilon T) \ < \ 1.1318 \times \varepsilon T(\delta 1 = 0),\\
0.4864 \times \varepsilon T(\delta 1 = 0) &< EX(\varepsilon T) < 1.2636 \times \varepsilon T(\delta 1 = 0). \qquad (A3.2b)
\end{aligned}$$

Changes in gap height occur successively with probabilities ranging from P_N = 0.6046 to P_N = 0.7884 and P_N = 0.9166 to P_N = 1.0000; as indicated on the vertical axis in Figure A3.2 a, b. Probability values P_n are highlighted in Figure A3.2 c, d. Based on the measurements illustrated in Figure A3.1, Fig.A3.2 a – Fig.A3.2 d, the following final forms of expected values of the lower and upper limits of the standard deviation interval of gap height between the spherical hip surfaces are derived [25-26]:

$$\varepsilon_T \times (1 + m^h - \sigma^h) = \varepsilon_T \times \sum_{i=s,n,N} P_i \cdot (1 + m_i - \sigma_i) =$$

$$= \varepsilon_T \cdot \{0.120 \cdot 0.5918 + 0.220 \cdot (0.8682 + 0.7364 + 0.3682 + 0.4864)\} = 0.6120 \cdot \varepsilon_T,\ (A3.3a)$$

$$\varepsilon_T \times (1 + m^h + \sigma^h) = \varepsilon_T \times \sum_{i=s,n,N} P_i \cdot (1 + m_i + \sigma_i) =$$

$$= \varepsilon_T \cdot \{0.120 \cdot 1.4082 + 0.220 \cdot (1.6318 + 1.5136 + 1.1318 + 1.2636)\} = 1.3879\varepsilon_T,\ \ A(3.3b)$$